

Probing the acid sites of zeolites with pyridine: quantitative AGIR measurements of the molar absorption coefficients

Vladimir Zholobenko ^{a,b} *, Cátia Freitas ^b, Martin Jendrlin ^b, Philippe Bazin ^a, Arnaud Travert ^a, Frederic Thibault-Starzyk ^a

^a Normandie Univ, ENSICAEN, CNRS, Laboratoire Catalyse et Spectrochimie, France

^b School of Chemical and Physical Sciences, Keele University, United Kingdom

Abstract

This study presents a detailed methodology, which combines high-precision thermogravimetry and FTIR spectroscopy, aiming to establish the most accurate and reliable means of measuring the molar absorption coefficients of adsorbed species. As the integrated molar absorption coefficients of Py complexes with Brønsted and Lewis acid sites, (Py-B) and (Py-L), are determined and the validity of the Beer-Lambert-Bouguer law for IR characterisation of solid acids is demonstrated, this work is setting a benchmark for the quantitative acidity measurements in zeolites and related materials. The following values of (Py-B) have been obtained at 150°C (band at ~1545 cm⁻¹): 1.09±0.08 cm μmol⁻¹ for ZSM-5; 1.12±0.16 cm μmol⁻¹ for BEA; 1.29±0.04 cm μmol⁻¹ for MOR and 1.54±0.15 cm μmol⁻¹ for FAU. The value of (Py-L) (band at ~1455 cm⁻¹, which refers to different cations) measured at the same temperature is 1.71±0.1 cm μmol⁻¹. Values of (Py-B) depend on the zeolite structure, in contrast to that for (Py-L). Clear correlations are presented between the temperature of the FTIR measurements and values for Py complexes and other species, which decrease by ~10% as the temperature increases by 100°C. In addition, the effects of key experimental procedures, instrumentation design and sample preparation are established and quantified.

Key words: zeolites; acid sites; FTIR; pyridine; molar absorption coefficients

* Corresponding author: v.l.zholobenko@keele.ac.uk

1. Introduction

Zeolites, particularly crystalline aluminosilicates, are essential for a host of major industrial processes. They are utilised as molecular sieves, for nuclear waste clean-up, as water softeners in washing powders, as vital catalysts in oil refining and petrochemical industries for the production of petrol and diesel, olefins and simple aromatic compounds, polymers and plastics, etc. The successful application of these materials in catalysis is associated with their microporous structure and highly effective acid sites. Hence, characterisation of the acidic properties of zeolites is of significant fundamental and practical importance. Over several decades, pyridine (Py) has been the most frequently utilised infrared probe molecule for the characterisation of active sites in solid acids [see review 1 and references therein]. Indeed, (i) Py complexes with acid sites can be easily discriminated in the spectra, thus Brønsted and Lewis acid sites (BAS and LAS) can be evaluated; (ii) Py is a rather stable molecule at a wide range of characterisation conditions, allowing for instance, high-temperature experiments, such as TPD; (iii) Py and its derivatives can be used to examine the accessibility of the acid sites in a variety of zeolite structures. In addition, FTIR spectra of adsorbed Py can be used for quantitative measurements of the number of acid sites present in a solid catalyst via the application of the Beer-Lambert law (this should be referred to as the Beer-Lambert-Bouguer law to acknowledge the original contribution by Pierre Bouguer). A wide range of molar absorption coefficient values can be found in the literature (Table 1) for Py adsorbed on BAS and LAS, (Py-B) and (Py-L). However, there are significant differences among the data published by different researchers: the values vary by six orders of magnitude, the (Py-B)/ (Py-L) ratios are between 0.47 and 8.8, and different units of are reported (Table 1), suggesting that such variations may be associated with significant errors [1]. Furthermore, the details of experimental procedures, which differ a great deal, and of the data analysis are frequently unclear or incomplete. In addition, the application of the classic Beer-Lambert-Bouguer law to the FTIR characterisation of solid catalysts is challenging, and the accuracy of quantitative data reported in the literature may be limited by the equipment available and the methodology utilised in such research. Indeed, the physical parameters and properties of the sample (its thickness, pressure used to prepare the disc, particle size, etc.) and the experimental design (spectral resolution, temperature of the FTIR measurements, using a vacuum system or a gas flow) may have a large influence on the values obtained [2]. It should be noted that for other probe molecules there are quantitative data in the literature, including the calculation of values for ammonia, quinoline, acetonitrile and substituted pyridines [1,3-8], but, these are not discussed in the present work.

Table 1. Molar absorption coefficients (ϵ) values for Py adsorbed on BAS and LAS reported in the literature.

Material	$\epsilon(\text{Py-B})$	Units	$\epsilon(\text{Py-L})$	Units	$\epsilon(\text{Py-B})/\epsilon(\text{Py-L})$	Resolution, cm^{-1}	Temperature, $^{\circ}\text{C}$	Year	Ref
Silica-alumina	-	-	-	-	$8.8 \pm 15\%$	2 or 4	-	1964	[9]
Silica-alumina	-	-	-	-	6.0 ± 9	-	-	1966	[10]
NH ₄ Y	3.03 ± 0.13	$\text{cm } \mu\text{mol}^{-1}$	3.26 ± 0.13	$\text{cm } \mu\text{mol}^{-1}$	0.93	-	150	1967	[11]
MOR	-	-	-	-	2.61	-	-	1968	[12]
MOR	-	-	-	-	1.54	4	-	1971	[13]
NaY	0.059 ± 0.004	$\mu\text{mol cm}^{-2}$	-	-	-	-	150	1980	[14]
NaHY	0.059 ± 0.004	$\text{cm}^2 \mu\text{mol}^{-1}$	0.084 ± 0.003	$\text{cm}^2 \mu\text{mol}^{-1}$	0.70	-	-	1981	[15]
ZSM-5	1.3×10^{-6}	$\text{cm } \mu\text{mol}^{-1}$	1.5×10^{-6}	$\text{cm } \mu\text{mol}^{-1}$	0.87	-	150	1986	[16]
Al ₂ O ₃ , Y	0.73	$\text{cm } \mu\text{mol}^{-1}$	1.11	$\text{cm } \mu\text{mol}^{-1}$	0.66	2	200	1992	[17]
MOR, ZSM-5, Y	1.67 ± 0.12	$\text{cm } \mu\text{mol}^{-1}$	2.22 ± 0.21	$\text{cm } \mu\text{mol}$	0.75	1	150 and 350	1993	[18]
BEA	1.3×10^{-6}	$\text{cm } \mu\text{mol}^{-1}$	1.5×10^{-6}	$\text{cm } \mu\text{mol}^{-1}$	0.87	-	30	1994	[19]
HY	1.8 ± 0.1	$\text{cm } \mu\text{mol}^{-1}$	1.5	$\text{cm } \mu\text{mol}^{-1}$	1.2	-	-	1994	[20]
Y	1.1	$\text{cm } \mu\text{mol}^{-1}$	-	-	-	2	30	1995	[21]
EMT	1.6	$\text{cm } \mu\text{mol}^{-1}$	-	-	-		30		
MOR	1.8	$\text{cm } \mu\text{mol}^{-1}$	-	-	-	2	30	1995	[22]
MOR, Y	0.078 ± 0.004	$\text{cm}^2 \mu\text{mol}$	0.269 ± 0.01	$\text{cm}^2 \mu\text{mol}$	0.29	-	145	1996	[23]
MOR, Al ₂ O ₃	1.13	$\text{cm } \mu\text{mol}^{-1}$	1.28	$\text{cm } \mu\text{mol}^{-1}$	0.88	-	-	1997	[24]
Y	0.085 ± 0.005	$\text{cm}^2 \mu\text{mol}$	-	-	-	-	145	1997	[25]

MAZ	1.13	cm μmol^{-1}	1.28	cm μmol^{-1}	0.88	-	-	1998	[26]
MCM-41	1.47	cm μmol^{-1}	1.98	cm μmol^{-1}	0.74	-	150	1999	[27]
BEA, MOR, Y, Silica-alumina	0.73 \pm 0.04	cm μmol^{-1}	0.64 \pm 0.04	cm μmol^{-1}	1.14	2	150	1999	[28]
Y	1.36 \pm 0.03	cm μmol^{-1}	-	-	-	4	200	2004	[29]
HMCM-41, Al₂O₃	0.070	cm μmol^{-1}	0.100	cm μmol^{-1}	0.70	2	150	2005	[30]
BEA, VBEA	0.070	cm μmol^{-1}	0.100	cm μmol^{-1}	0.70	2	150	2006	[31]
MCM-48, MCM-68	0.078	cm μmol^{-1}	0.165	cm μmol^{-1}	0.47	2	170	2010	[32]
Silica-alumina	0.57	cm μmol^{-1}	1.5	cm μmol^{-1}	0.38	-	-	2010	[33]
SBA-15	1.67 \pm 0.12	cm μmol	2.22 \pm 0.21	cm μmol	0.75	4	30	2010	[34]
Silica-alumina	1.67 \pm 0.12	cm μmol	2.22 \pm 0.21	cm μmol	0.75	4	150	2012	[35]
HY	1.95 \pm 0.13	cm μmol^{-1}	1.45 \pm 0.10	cm μmol^{-1}	1.34	2	150	2016	[36]
SnBEA	-	-	1.42 \pm 0.30	cm μmol^{-1}	1.37				
SAPO-34	0.06	cm ² μmol^{-1}	-	-	-	4	-	2017	[37]
ZSM-5	0.07	cm ² μmol^{-1}	0.10	cm ² μmol^{-1}	0.70	2	170	2017	[38]
BEA	1.98 \pm 0.16	mmol/g _{cat} /area	2.53 \pm 0.38	mmol/g _{cat} /area	0.78	4	30	2018	[39]
ZSM-5	2.98 \pm 0.49		~2.2		1.35				
Y	2.55 \pm 0.28		2.27 \pm 0.41		1.12				

Significant advances in the design of new instrumentation for the accurate quantitative analysis of the FTIR spectra have been made in the last few years [7,29,40], such as the combination of high-precision thermogravimetry and FTIR spectroscopy (AGIR, combining gravimetric analysis and IR). This technique, in which a microbalance is integrated with an FTIR in situ cell within a single set-up, allows simultaneous monitoring of the weight changes of the sample along with its IR spectra during adsorption or desorption of probe molecules, and consequently, highly accurate quantitative data, e.g. the molar absorption coefficient values, can be obtained directly, as demonstrated in [41-43]. The aim of this work is to carry out quantitative analysis of the number of acid sites in different zeolites, to determine the value of the integrated molar absorption coefficients of Py adsorbed on Brønsted and Lewis acid sites and to examine the role of experimental conditions that are essential for the reliable characterisation of the acidic properties of zeolite-based catalysts. This study also examines the validity of the Beer-Lambert-Bouguer law in solid materials. The (Py-B) and (Py-L) values have been determined using the AGIR technique, which, we believe, is the most accurate and reliable method of measuring the molar absorption (extinction) coefficients of adsorbed species. Overall, the optimisation of the experimental procedures is imperative for the successful quantitative evaluation of different types of acid sites in zeolitic materials. With the new level of instrumentation available now, this work sets a benchmark for the quantitative acidity measurements in zeolites and related materials.

2. Experimental

Materials. Ammonium forms of zeolites BEA-12 (CP814E, Zeolyst International, Si/Al=12.5), BEA-19 (CP814C, Zeolyst International, Si/Al=19) ZSM-5-40 (MFI structure type, CBV8014, Zeolyst International, Si/Al=40), ZSM-5-27 (MFI structure type, NIST reference material RM8852, Si/Al=27 [44]), MOR-7 (Crosfield, Si/Al=7.0), MOR-10 (CBV21A, Zeolyst International, Si/Al=10) FAU-C (Crosfield, Si/Al=2.6), FAU-Z (CBV300, Zeolyst International, Si/Al=2.6), -alumina (Puralox, Sasol) and fumed silica (SiO₂, Sigma-Aldrich, 99.8%) were either used as received or calcined ex situ at 450-900°C in a muffle furnace for 5 hours. This procedure allowed to obtain materials from the same type of the zeolite framework but with different BAS/LAS ratios. In addition, a sample of US-Y zeolite (Crosfield, Si/Al=6) was used in this group of samples. All the parent zeolites are readily available commercial samples, whose XRD patterns, textural properties, SEM and TEM images, NMR and FTIR spectroscopic data can be found in the literature. To account for the potential batch to batch variations and the differences in the methodologies applied by various research groups, characterisation data for the samples studied in this work are presented in the Appendix of the Supplementary Information section (SI).

In situ FTIR experiments. An in situ IR cell was attached to a vacuum system (dynamic vacuum better than 10⁻⁵ mbar) and the FTIR measurements were carried out using a Thermo iS10

FTIR spectrometer, equipped with a DTGS detector, in the range 6000-1000 cm^{-1} at a spectral resolution of 1-8 cm^{-1} (typically 4 cm^{-1}) and 64 scans in transmission mode (Figures 1 and S1). Prior to recording the spectra, a self-supported sample disk (1.3 cm in diameter, $S=1.3 \text{ cm}^2$; 1.5 to 30 mg/cm^2 , but typically 7-10 mg/cm^2) was activated in the *in situ* vacuum cell typically at 450°C (ramp 1°C/min). After a period of 5 hours at the selected activation temperature, the sample was cooled to the desired temperature (between 50 and 350°C) in vacuum and its IR spectrum was collected. Small portions of the probe molecule, Py ($\text{C}_5\text{H}_5\text{N}$, Acros Organics, 99.5%, dried over 3A molecular sieve), were admitted into the cell, usually at 150°C, until no changes in the peak intensities were observed in the spectra. Physisorbed molecules were subsequently removed by evacuation at 150°C. Py adsorption-desorption was carried out typically at 150-350°C. The FTIR spectra were collected at different temperatures, typically between 50 and 350°C. The obtained spectra were analysed, including integration, subtraction and determination of peak positions, using specialised Thermo software, Omnic. The integration limits were 1565 to 1515 cm^{-1} for the Py-B peak and 1465 to 1535 cm^{-1} for the Py-L peak ($\pm 3 \text{ cm}^{-1}$ depending on the nature of the sample and the temperature of the FTIR measurements).

CARROUCELL experiments. The statistical CARROUCELL experiments were performed in a specially designed *in situ* cell, attached to a vacuum system accommodating up to 12 samples (Figure 1). 10 self-supported sample disks (1.6 cm in diameter, $S=2.0 \text{ cm}^2$; $\sim 10 \text{ mg}/\text{cm}^2$) were activated under vacuum at 450°C for 5 hours (ramp 1°C/min). FTIR spectra of the samples before and after Py adsorption were recorded at 30-450°C using a Thermo iS50 FTIR spectrometer equipped with an MCT detector, at a spectral resolution of 4 cm^{-1} . The zeolite samples were prepared by different researchers to test the operator effect on the quality of the data. In addition, FTIR measurements for every sample were repeated using a second round of the CARROUCELL (the time delay between the two rounds was ~ 30 minutes) to evaluate the instrumentation effect on the data quality.

AGIR experiments. With the AGIR set-up, the mass (and therefore the number of adsorbed molecules) and FTIR spectra of the sample can be measured simultaneously in real-time in a gas flow system at temperatures between 30 and 500°C (Figures 1 and S2) [7]. The analyses were carried out on self-supported discs ($\sim 20 \text{ mg}$, 1.6 cm in diameter, $S=2.0 \text{ cm}^2$), which were activated in the IR reactor-cell at 450°C under a flow of Ar for 5 h (ramp 1°C/min). FTIR spectra of the samples were recorded at 30-450°C every 300 seconds using a Thermo Nicolet 6700 spectrometer equipped with an MCT detector, typically at a spectral resolution of 4 cm^{-1} (Figure S2). The mass changes of the same sample were continuously monitored by a SETSYS-B Setaram microbalance (the temporal resolution of ~ 10 sec and accuracy of the mass measurements better than $\pm 1 \text{ }\mu\text{g}$) and the gas flow composition was analysed by a Pfeiffer Omnistar GSD301 mass-spectrometer.

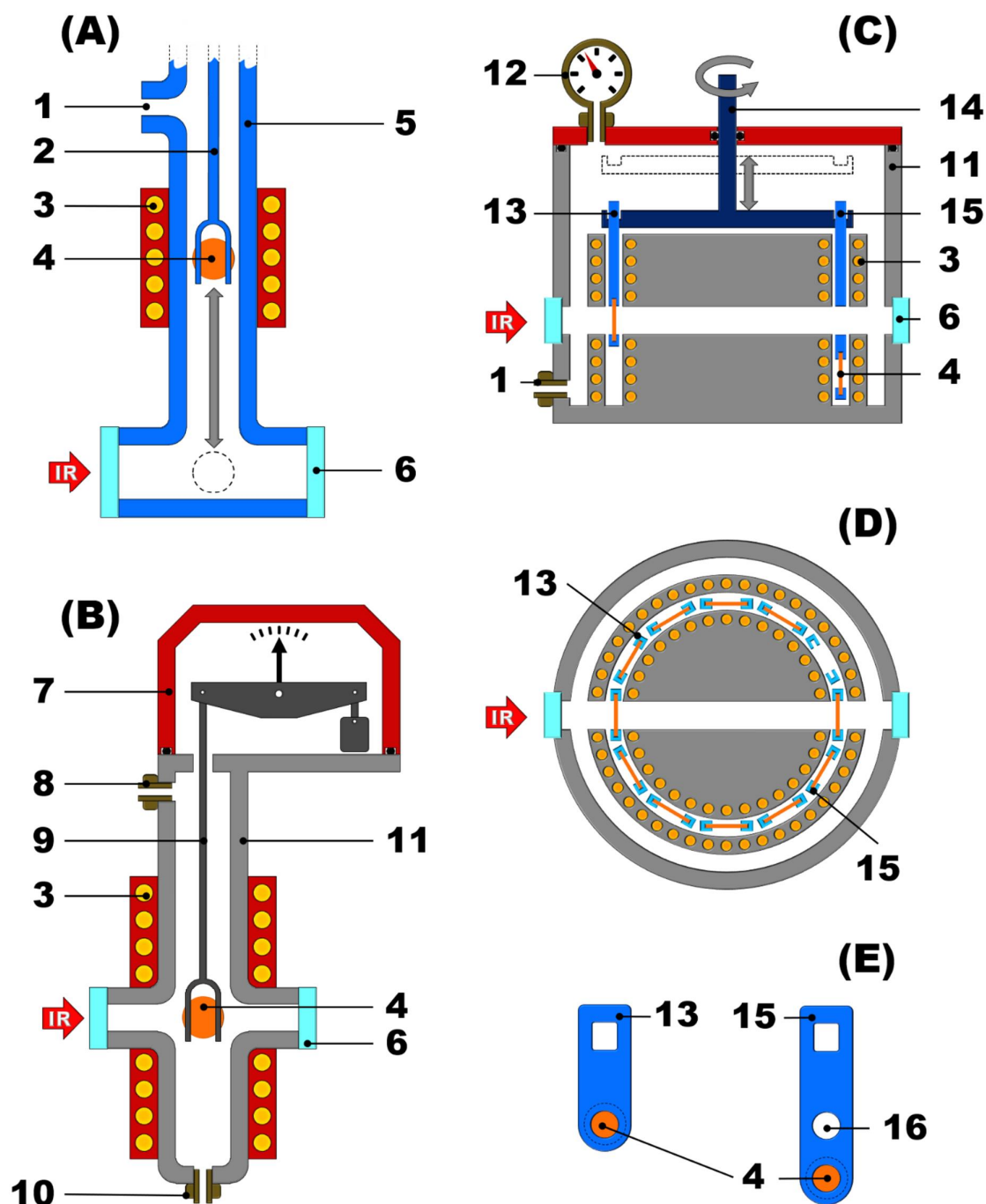


Figure 1. Schematics of the IR cells used in this work: (A) classical in situ IR cell (bottom part), (B) AGIR set-up, (C) longitudinal and (D) top (scale = 0.5) views of the CARROUCELL cell and (E) CARROUCELL sample holders. 1 - connection to the vacuum set-up, 2 - sample holder (quartz), 3 - heating element, 4 - sample disc, 5 - body of the cell (quartz), 6 - KBr window, 7 - head of the microbalance, 8 - inlet gas connection, 9 - sample holder (stainless steel), 10 - outlet gas connection, 11 - body of the cell (stainless steel), 12 - pressure gauge, 13 - small sample holder (quartz), 14 - rotating rack for 12 sample holders (in stainless steel), 15 - high sample holder (quartz), 16 - through-hole for the IR beam.

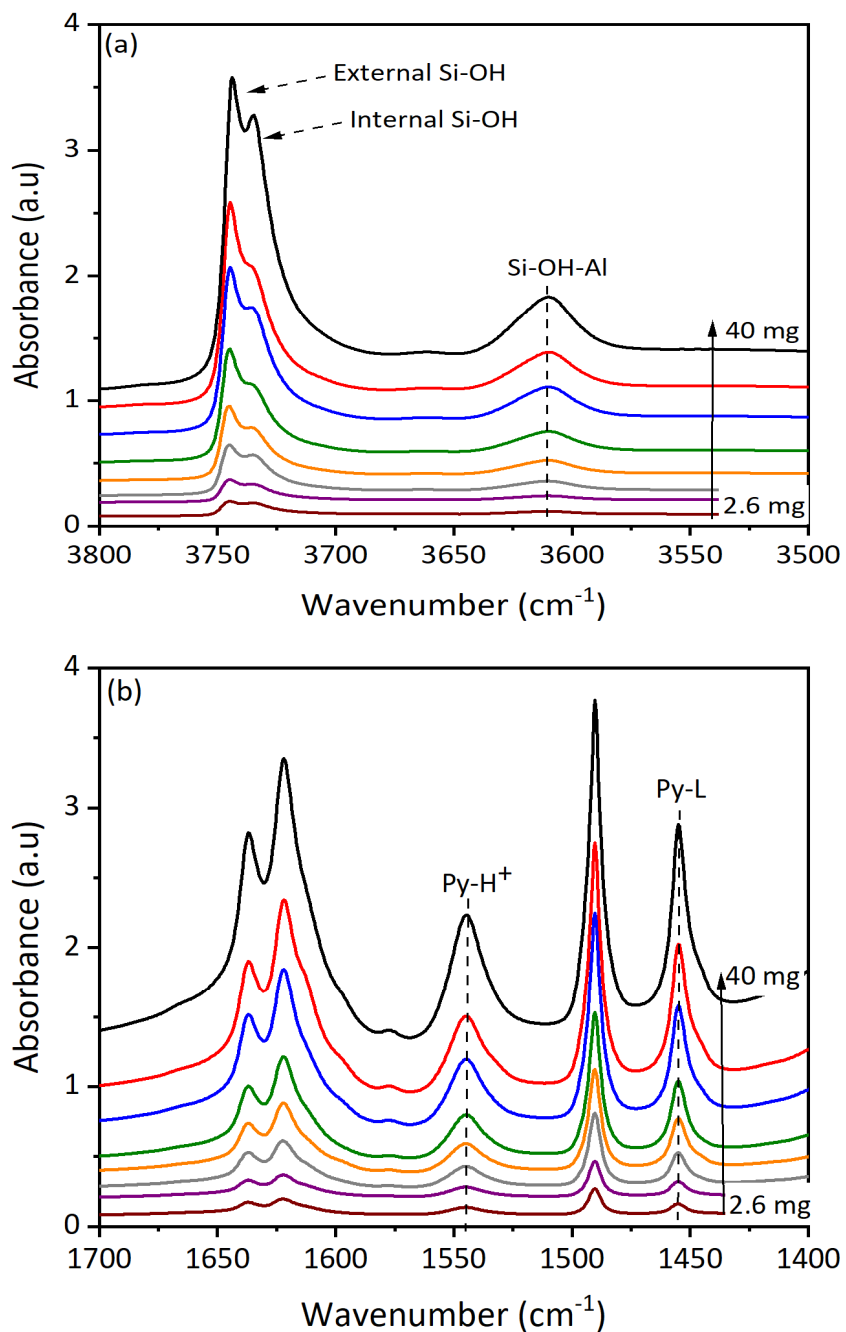
82

83 **3. Results and Discussion**

84 Preliminary work carried out to check the validity of the Beer-Lambert-Bouguer law for the
85 FTIR characterisation of zeolites and to illustrate the effects of the preparation procedure on
86 quantitative measurements is presented in SI (this includes the initial titration-style FTIR
87 measurements and a SEM examination of the self-supported IR discs, Figures S3-S6). The acid site
88 titration experiments involve admitting small doses of Py into the in situ IR cell while changes in
89 the intensity of the IR peaks are monitored. FTIR spectra of the activated BEA zeolite show major
90 peaks in the OH-region at 3745 cm^{-1} , with a shoulder at $\sim 3735\text{ cm}^{-1}$, which are attributed to the
91 external and internal Si-OH groups, and at 3610 cm^{-1} assigned to the acidic bridging Si-OH-Al
92 groups (Figure 2). The interaction of Py with the zeolite leads to a decrease in the intensity of the
93 Si-OH and Si-OH-Al bands and gives rise to the following sets of peaks: two peaks at ~ 1545 ($_{19b}$)
94 and 1637 ($_{8a}$) cm^{-1} due to pyridinium ions resulting from Py protonation on Brønsted acid sites
95 (Py-B complexes, i.e. protonated Py, Py-H^+), two peaks assigned to Py coordinated to Lewis acid
96 sites (Py-L complexes) at ~ 1456 ($_{19b}$) and 1622 ($_{8a}$) cm^{-1} and overlapping signals of Py on Lewis
97 and Brønsted acid sites at ~ 1491 ($_{19a}$) cm^{-1} . In the presence of H-bonded and physisorbed Py,
98 additional peaks or shoulders are observed in the spectra, at ~ 1595 and 1580 cm^{-1} for the $_{8a}$ mode,
99 as well as at ~ 1445 and 1438 cm^{-1} for $_{19b}$. The low-intensity peak, detected at 1580 cm^{-1} after the
100 removal of physisorbed Py, can be attributed to the $_{8b}$ mode of Py-L complexes.

101

102



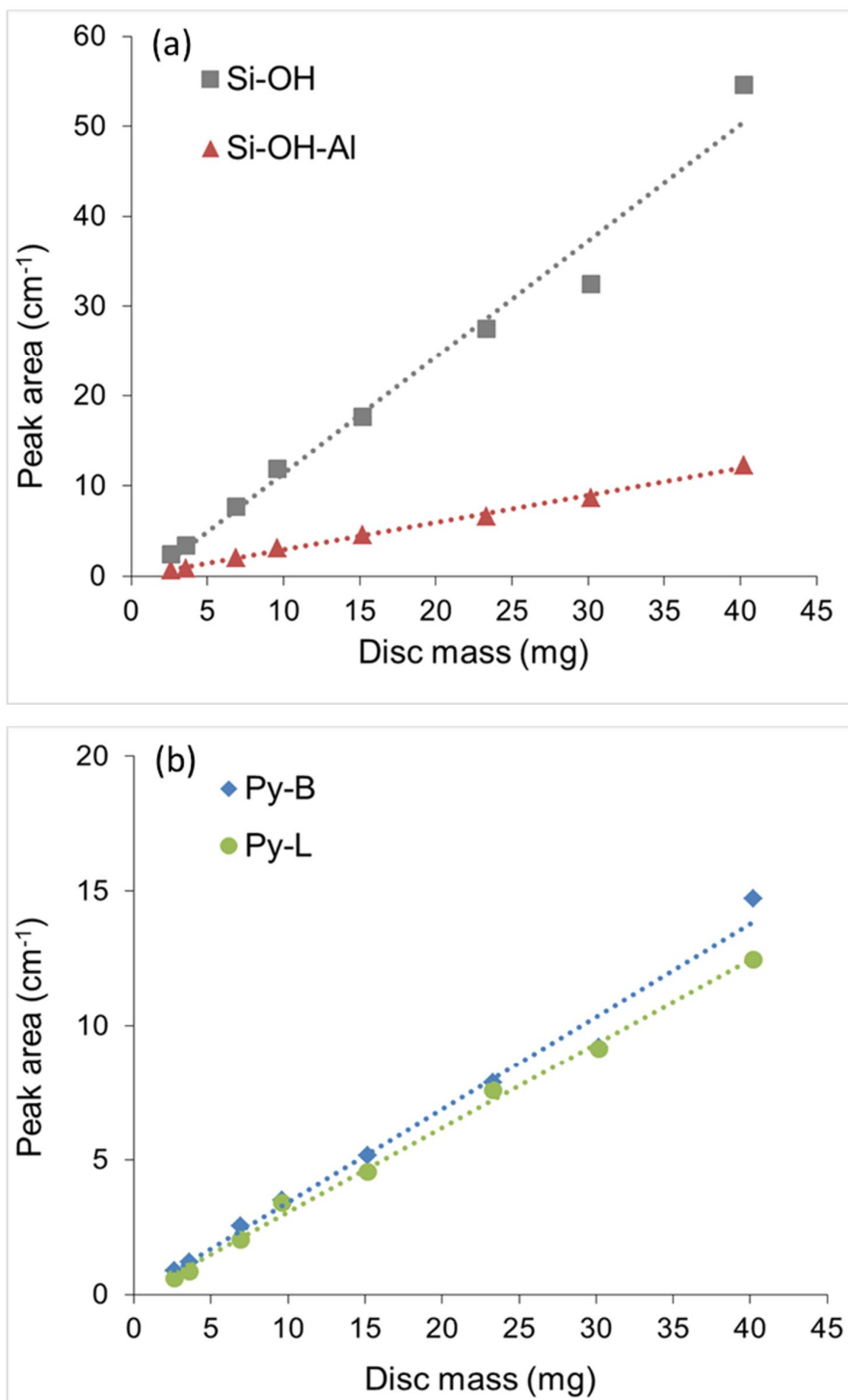
104 **Figure 2. (a)** FTIR spectra of the OH-region prior to Py adsorption and **(b)** difference FTIR spectra
 105 of the Py region following Py adsorption at 150°C collected on BEA-12 discs of different mass (~2-
 106 40 mg, 1.3 cm in diameter, $S=1.3 \text{ cm}^2$; spectra collected at 90°C).

107

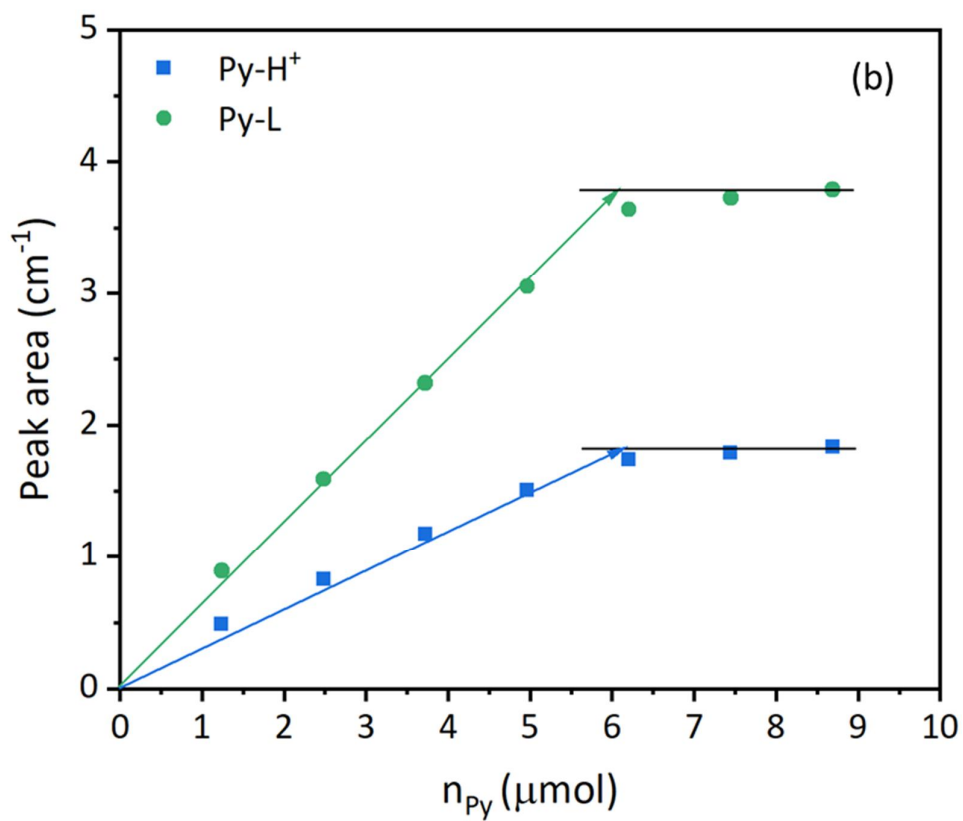
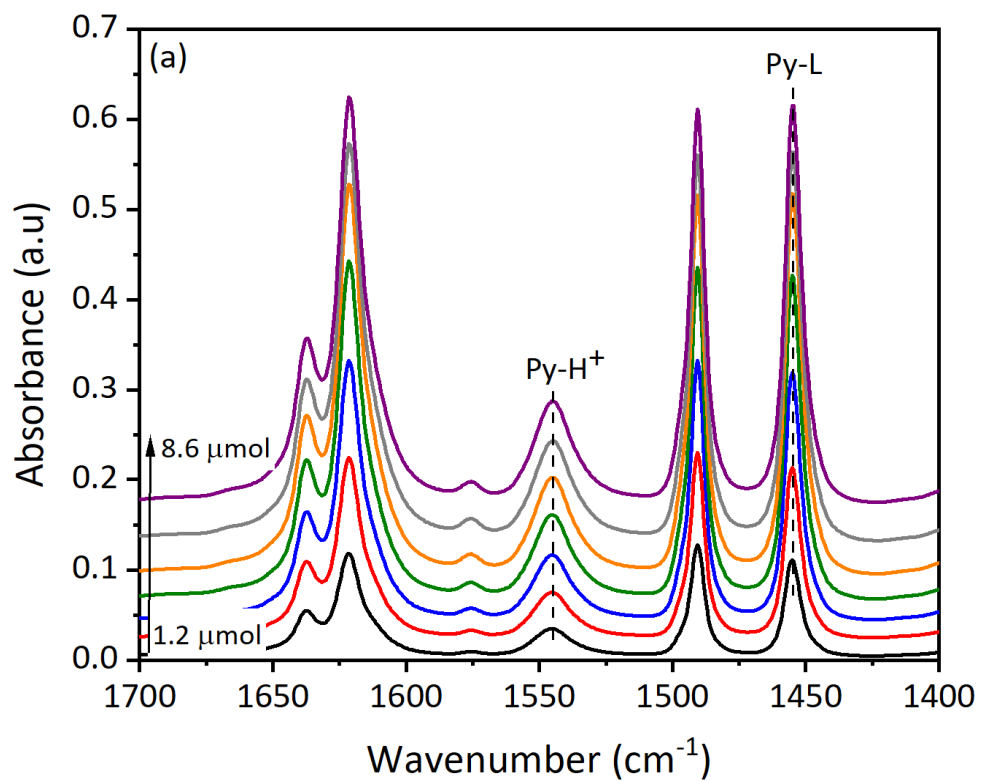
Next, the effect of the sample mass, which is used as a proxy for the effective sample pathlength, on the intensity of the IR peaks has been investigated. The quantitative data obtained (e.g. Figure 2) have been used to validate the Beer-Lambert-Bouguer law. The intensities of the peaks of Si-OH-Al ($\sim 3610\text{ cm}^{-1}$), Si-OH ($\sim 3745\text{ cm}^{-1}$) groups, Py-B ($\sim 1545\text{ cm}^{-1}$) and Py-L ($\sim 1456\text{ cm}^{-1}$) complexes increase with the sample mass (Figures 2 and 3). The data show a clear linear relationship between absorbance (measured either as the peak area or peak height) and the mass of the discs, demonstrating that the Beer-Lambert-Bouguer law is valid for solid materials in IR spectroscopy (Figures 3 and S5), although, some noticeable deviation from it is observed for samples heavier than 25 mg (i.e. $>20\text{ mg/cm}^2$; Figure S6). For practical FTIR measurements, the sample size between 5 and 15 mg/cm^2 should be recommended. Our results demonstrate that the sample preparation and activation procedures need to be carefully controlled in order to obtain quantitative data. Although the experimental data confirm the validity of the Beer-Lambert-Bouguer law for solid materials, these measurements have been performed with a BEA zeolite with low scattering in the mid-IR range. For materials which strongly scatter IR radiation, the sample density should be limited to $\sim 10\text{ mg/cm}^2$ to ensure both good quality and quantitative nature of the FTIR measurements. It is important to note that the pressure applied while making the self-supporting discs should be kept to a minimum, certainly below 0.5 tones/cm^2 , as a higher pressure can lead to the incomplete sample activation (see Figure S7 and related comments) and structural degradation in extreme cases.

The results of statistical CARROUCELL experiments carried out on five ZSM-5-40 and five BEA-12 samples are presented in Figures S8-S10 and Table S1. The data demonstrate that for the in situ FTIR measurements, the instrumentation errors are within $\pm 1\%$, whereas those associated with the sample preparation (the *ö*operator effect \ddot{o}) can be around $\pm 10\%$. The overall error can be reduced to about $\pm 5\%$ by carrying out repeated measurements (5 samples in this work).

Following the traditional titration-style experiments (Figure 4), a linear relationship has been obtained between the amount of Py introduced and the changes in the peak intensities, e.g. at $\sim 1545\text{ cm}^{-1}$ for Py-B and at $\sim 1456\text{ cm}^{-1}$ for Py-L complexes following the first few injections. When all sites are saturated, Py is no longer adsorbed on BAS and LAS, hence a plateau is observed and the number of acid sites can be calculated from the titration graph. It should be noted that the amount of Py interacting with acid sites is determined from the titration experiments with a degree of uncertainty as some Py is likely to be adsorbed on the walls of the IR cell and the vacuum system. The best way to minimise this uncertainty is to measure the mass of the sample during Py adsorption-desorption and monitor its FTIR spectra at the same time in a single experiment, which is achieved by the AGIR methodology.

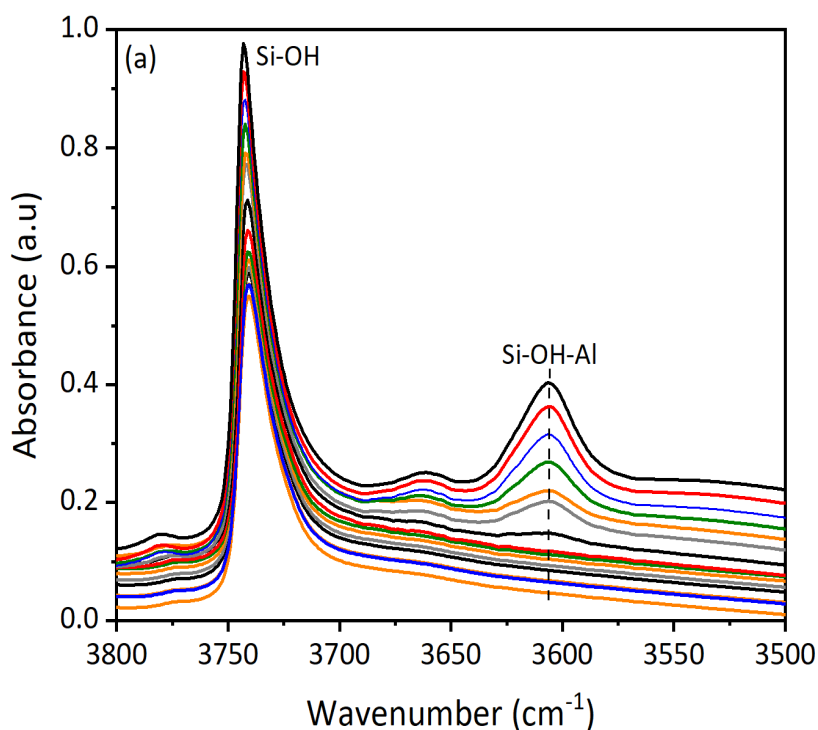


144 **Figure 3.** Linear relationship between the zeolite disc mass and the integrated absorbance of the IR
 145 bands of (a) OH groups and (b) Py adsorbed on BAS and LAS in BEA-12 zeolite.
 146



147 **Figure 4.** Zeolite BEA-12-600°C: titrations of BAS and LAS with Py at 150°C. (a) Difference FTIR
 148 spectra of the Py region. (b) Integrated peak area as a function of the increasing amount of added Py
 149 (spectra collected at 90°C).

Figure 5 presents an example of AGIR data collected following Py adsorption-desorption on a sample of BEA-12. The integration of a microbalance and an infrared in situ flow-cell in a single set-up affords simultaneous monitoring of the weight changes (TG signal) of the sample and the spectra acquisition (FTIR signal). The temporal resolution of the TG analysis in this work is ~10 seconds and that for the FTIR measurements is ~30 seconds (both could be improved by a factor of ~10 if required). As the accuracy of the mass measurements is better than $\pm 1 \mu\text{g}$ and a typical amount of Py adsorbed is between 100 and 2000 μg per sample, highly accurate measurements of the molar absorption coefficients of adsorbed Py species can be achieved from the combination of the TG and FTIR data. In general, the spectroscopic data acquired using this methodology are in agreement with the spectral observations obtained by in situ FTIR, that is Py adsorption at 150°C on BEA-12 leads to the formation of peaks at ~ 1545 and $\sim 1455 \text{ cm}^{-1}$ corresponding to Py-B and Py-L complexes (spectra of other zeolites before and after Py adsorption are provided in the Appendix of the SI section). However, when the dynamic TG and FTIR signals are overlaid, they do not coincide, showing a time lag of ~5 minutes (Figure S11), whereas the MS monitoring the downstream concentration of Py confirms a typical break-through chromatographic behaviour of the zeolite sample in the AGIR cell. Therefore, any quantitative kinetic type measurements in any similar system, e.g. time-resolved diffusion or adsorption experiments, should be carried out with great care. All the AGIR data utilised in this work for the calculation of (Py-B) and (Py-L) have been obtained following Py desorption, rather than adsorption, allowing for the system equilibration for at least 20 minutes.



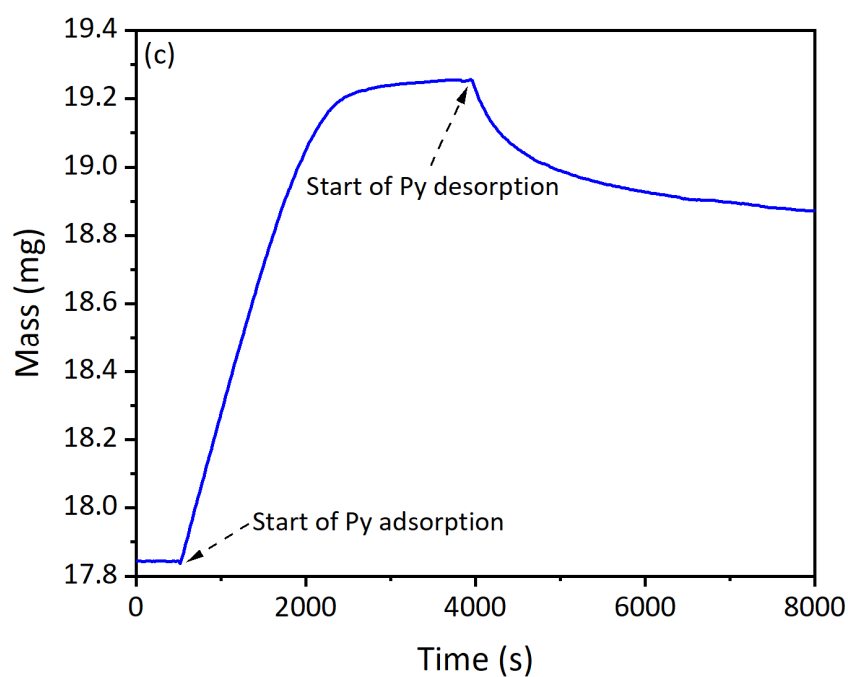
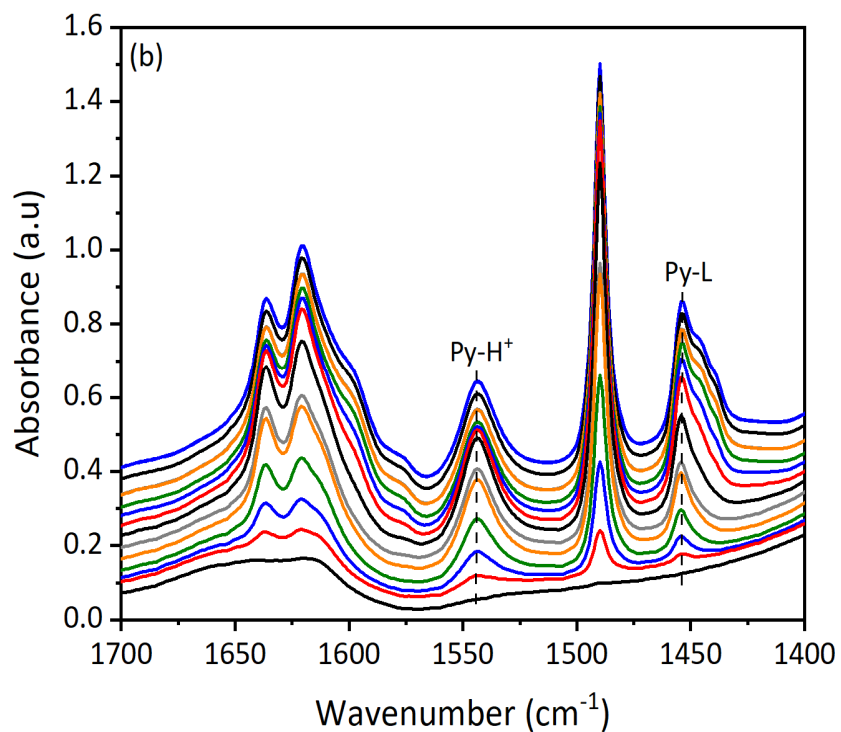


Figure 5. FTIR spectra of the (a) OH-region and (b) Py region following Py adsorption at 200°C on BEA-12 and (c) TGA data obtained on BEA-12 in the course of the AGIR experiment (data collected at 200°C).

Effect of physisorbed Py species.

Py adsorption on zeolites is typically performed at 30-150°C followed by the removal of physisorbed Py species, which are held on the zeolite surface by weak hydrogen-bonding and van-der-Waals interactions giving rise to the peaks at 1585-1595 and 1438-1445 cm^{-1} [1,45]. The effect of physisorbed Py on the intensity of the IR bands is exemplified by the spectra obtained for BEA-12 zeolite after Py desorption at 200°C (Figure 6). Over ~60 minutes, the intensity of the peak shoulder at ~1440 cm^{-1} decreases, indicating that the physisorbed Py species are being removed at 200°C. At the same time, the TG signal shows a ~27% decrease (from 850 to 615 $\mu\text{mol/g}$), but the intensity of the peak corresponding to Py-B species at ~1545 cm^{-1} increases by ~25%. These observations can be explained by a δ solvent δ effect, as weakly bound Py molecules reduce the transient dipole moment of the protonated Py- H^+ species (probably, by forming $\text{Py}\cdots\text{Py-H}^+$ complexes, in which the N-atom of the Py molecule forms a H-bond with the pyridinium ion) that would cause a decrease in the value of (Py-B). Py is not the only basic test-molecule, for which analogous δ solvent δ effect has been detected. Indeed, similar observations have been reported for ammonia adsorption on H-forms of zeolites ZSM-5, BEA, MOR and Y with the formation of $[\text{NH}_4\cdots\text{NH}_3]^+$ dimers and their subsequent solvation by excess ammonia [46]. Our data demonstrate that the removal of physisorbed Py species should be conducted preferably at 200°C (150-200°C depending on the zeolite) by purging or evacuation and should be monitored to ensure the one-to-one interaction between Py and BAS, and hence, the accuracy of acidity measurements.

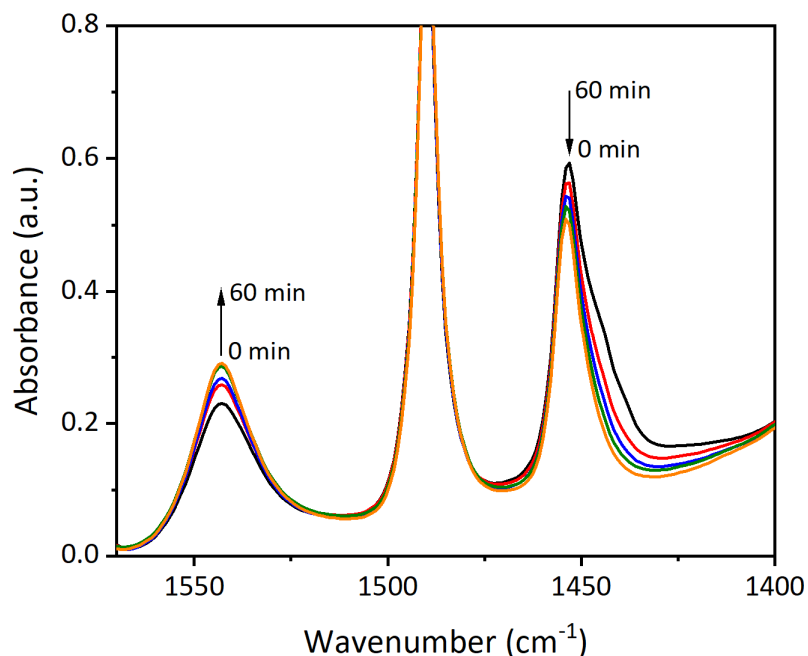


Figure 6. Difference FTIR spectra of Py adsorbed at 200°C on BEA-12 zeolite after desorption over 60 min (spectra collected at 200°C; the arrows indicate an increase or decrease in the intensity of IR peaks).

Effect of the spectral resolution.

The effect of resolutions on Py-B and Py-L peaks has been studied for BEA-19 following Py adsorption at 150°C (Figure S12 and Table S2). Significant differences can be observed in the shape and intensity of the Py-B, and particularly, the Py-L peaks. This can be attributed to the greater width of the Py-B peak (FWHH~16 cm⁻¹) as compared to that for Py-L (FWHH~7 cm⁻¹). The calculation of the peak intensities reveals noticeable potential experimental errors associated with collecting the spectroscopic data at different resolutions, especially when the measurements are done by the peak height (~17% for Py-L at 4 cm⁻¹ resolution, see Table S2). Table 1 shows significant differences in the experimental approaches described in the literature, including the resolution at which the IR spectra are obtained. A rather common resolution used is 4 cm⁻¹, however, the values do vary, and frequently are not mentioned at all, which could be one of the factors leading to discrepancies in the reported data. Clearly, it is best to compare the results obtained under the same conditions, but if this is not possible, it is advisable to use calculations based on peak area instead of peak height, or to apply correction values provided in Table S2.

Effect of the temperature.

Our experimental data demonstrate that the temperature of the FTIR measurements has a significant effect on the calculated values (Figure 7). With the increase in the temperature of the sample under examination, both Py-B and Py-L bands are red-shifted, they become broader and their intensity decreases (both the peak height and peak area). For instance, as the temperature of the sample in the IR cell increases by 100°C, the Py-B peak shifts by ~2 cm⁻¹ and the Py-L peak shifts by ~1 cm⁻¹ and their peak areas, and hence the measured value of the integrated molar absorption coefficients, decrease by ~10% (the effect is reversible as the measurement temperature is increased or decreased). The results, obtained for ZSM-5, BEA, FAU and MOR zeolites and summarised in Figure S13 and Tables S3 and S4, provide clear experimental evidence that (Py-B) and (Py-L) values do depend on the temperature of the FTIR measurements, which disagrees with previous assumptions [13,18]. Furthermore, as indicated in Table 1, the experimental temperature of the data collection is not specified in many published reports, which can introduce yet another source of uncertainty in the calculation of the number of acid sites in zeolite-based catalysts if random literature data for the molar absorption coefficients are used. It should be noted that similar effects are observed for the isolated OH-groups in all studied zeolites (both the red-shift and a decrease in the peak area at higher temperatures). As the temperature of the FTIR measurements is increased by 100°C, the Si-OH peak shifts by ~2 cm⁻¹ and peak of the bridging OH-groups shifts by ~4 cm⁻¹, accompanied by a 10-15% decrease in the peak area (Table S4).

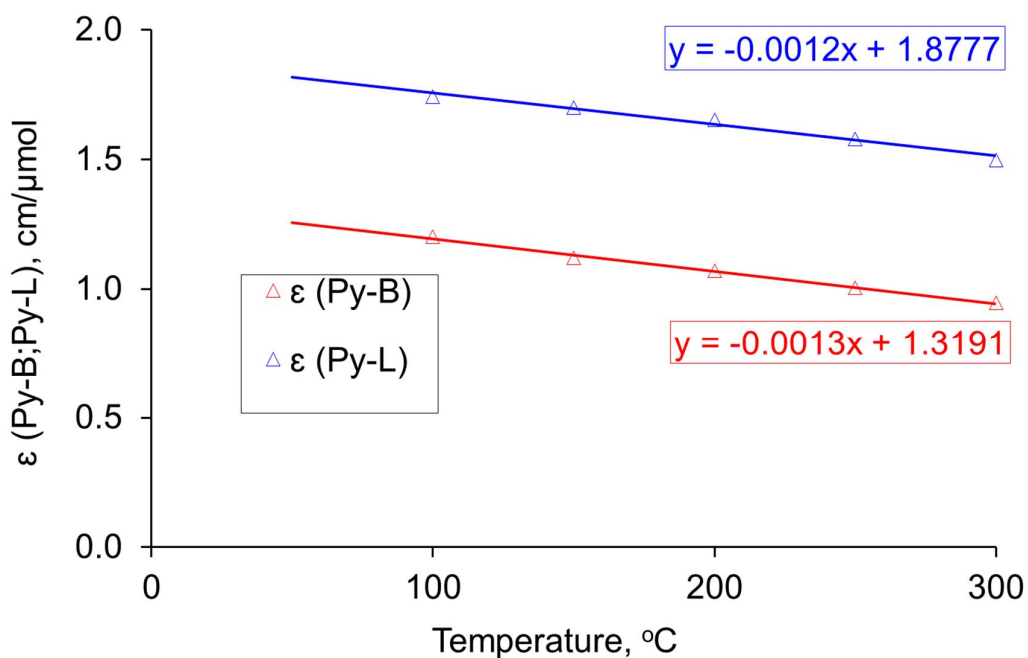
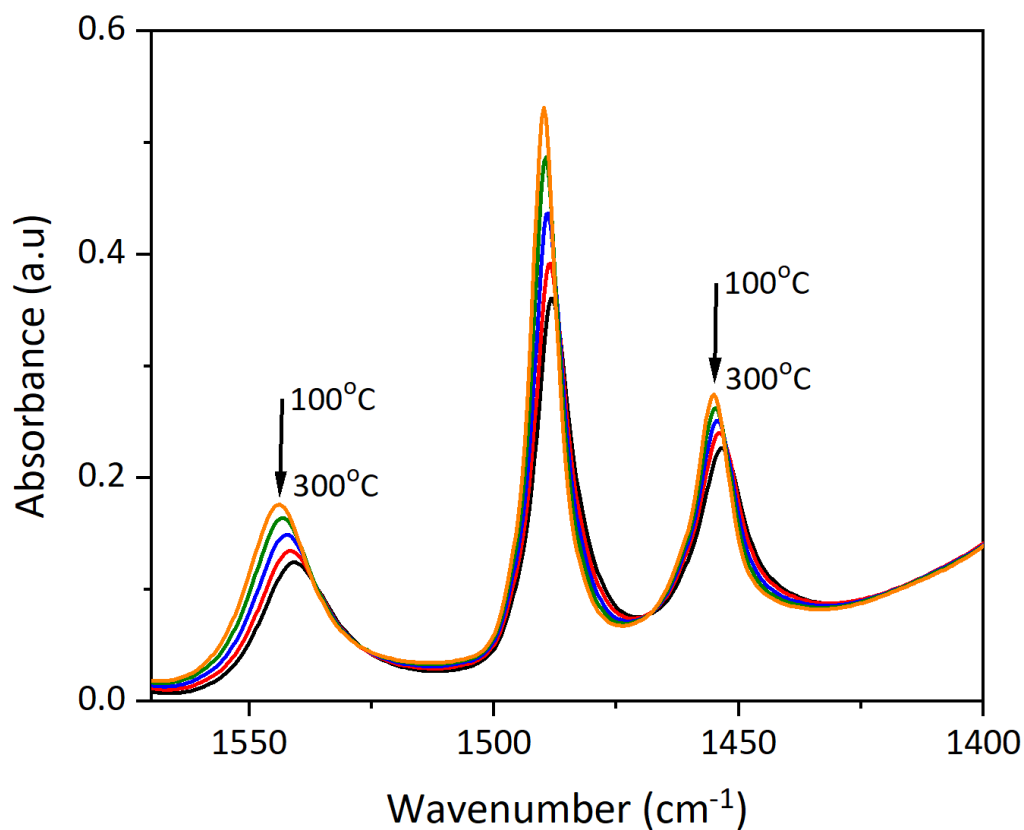


Figure 7. (a) FTIR spectra of Py adsorbed on BEA-12. Py was adsorbed at 150°C and then desorbed at 350°C; next, the sample temperature was decreased and the spectra collected at 100-300°C. (b) Molar absorption coefficients of Py-B and Py-L complexes for BEA-12 as a function of temperature of the FTIR measurements.

The modified Beer-Lambert-Bouguer law (Equation 1), which is commonly used in FTIR research on solid acid catalysts, allows the calculation of the ϵ values when the total amount of Py introduced and the intensity of the peak (Py-B or Py-L) are known.

$$A = \epsilon \frac{n^{Py}}{S} \quad (1)$$

where n^{Py} is the number of Py species (in μmol) in the sample disc, A is the peak area (in cm^{-1}) and S is the cross-section area of the zeolite disc ($S=1.3 \text{ cm}^2$ for in situ studies and $S=2.0 \text{ cm}^2$ for AGIR experiments). For each material under investigation, the integrated areas of the peaks corresponding to Py adsorbed on BAS and LAS and n^{Py} values (obtained from the TG signal and utilised to determine the number of BAS and LAS, Table 3) have been used to calculate ϵ (Py-B) and ϵ (Py-L) according to Equation 1 using a number of repeat experiments. The data obtained at different temperatures for zeolites ZSM-5, BEA, MOR and FAU are summarised in Tables 2 and S3 and Figure S13. An important conclusion, which can be drawn from these data, is that the ϵ (Py-B) values are dependent on the zeolite structure, whilst the ϵ (Py-L) values are very similar even for different types of LAS.

Table 2. Values of the integrated molar absorption coefficients for Py-B and Py-L complexes on various zeolites determined from the AGIR and in situ experiments.

Sample	ϵ (Py-B)*, $\text{cm}/\mu\text{mol}$			ϵ (Py-L)*, $\text{cm}/\mu\text{mol}$		
	30°C	150°C	200°C	30°C	150°C	200°C
-Al ₂ O ₃				1.87±0.1	1.71±0.1	1.65±0.1
ZSM-5 Si/Al=27-40	1.23±0.08	1.09±0.08	1.05±0.08			
BEA Si/Al=12-19	1.26±0.16	1.12±0.16	1.07±0.15			
MOR Si/Al=10	1.38±0.04	1.29±0.04	1.23±0.04			
FAU Si/Al=2.6	1.65±0.15	1.54±0.15	1.46±0.15			
CaZSM-5 Si/Al=40				1.87±0.2	1.71±0.2	1.64±0.2
NaZSM-5 Si/Al=40				1.88±0.2	1.72±0.2	1.65±0.2

* (Py-B) and (Py-L) data reported for 200°C are experimental AGIR values and those for 30°C and 150°C are obtained by extrapolation and verified using in situ experiments.

Table 3. The number of BAS and LAS obtained for the studied zeolites from AGIR experiments.

Sample	BAS, $\mu\text{mol/g}$	LAS, $\mu\text{mol/g}$
-Al ₂ O ₃	-	125
ZSM-5-40	325	10
ZSM-5-27	450	10
BEA-12	495	120
BEA-19	485	65
MOR-10	970	5
FAU-C	1080	20

* BAS and LAS data reported are experimental AGIR values obtained following Py desorption at 200°C. Not all acid sites are accessible in MOR and FAU zeolites.

Analysis of the experimental data for the samples containing both BAS and LAS.

As zeolites often have both BAS and LAS, the relationship between the amount of Py interacting with acid sites and the molar absorption coefficient values is given by the following equations:

$$n_{total}^{Py} = n_B^{Py} + n_L^{Py} \quad \text{or} \quad (2)$$

$$n_{total}^{Py} = \frac{A_B \times S}{\epsilon_B} + \frac{A_L \times S}{\epsilon_L} \quad (3)$$

Equation 3 contains two unknown parameters (ϵ_B and ϵ_L , these stand for (Py-B) and (Py-L)) and in a single experiment it is not possible to determine both of them. Therefore, it is necessary to use zeolites with different BAS/LAS ratios (zeolites calcined at four different temperatures have been used in this work). Then, the calculation of both ϵ_B and ϵ_L can be achieved by applying a linearised form of Equation 3 shown below.

$$\frac{A_B \times S}{n_{total}} = -\frac{\epsilon_B}{\epsilon_L} \times \frac{A_L \times S}{n_{total}} + \epsilon_B \quad (4)$$

Using Equation 4, both (Py-B) and (Py-L) values can be determined from the slope and the y-intercept of the trend line. Indeed, a similar approach has been suggested previously [18,39] based on the assumption that (Py-B), as well as (Py-L) values, are the same for different solid acid catalysts. Although both (Py-B) and (Py-L) can be calculated from FTIR *in situ* experiments, our data presented in Tables 2 and S3 and Figures S13 and S14 clearly demonstrate that the (Py-B) values are dependent on the zeolite structure, which contradicts the earlier conjecture made in the

literature [18,39]. In addition, this approach leads to a significant variation in calculated values of the molar absorption coefficients, particularly for the Py-L complexes. This is related to the fact that the accuracy of the suggested model is strongly dependent on the experimental parameters. Firstly, from the results presented in Figure S14, it is self-evident that if data for different zeolites are grouped together, then the $\bar{\epsilon}$ values of (Py-B) and (Py-L) would be determined by the choice of the selected or available experimental data points, and hence, would be different for different investigations, if the data for different zeolite types are indeed combined in such investigations. Secondly, an important limitation of this model is the potentially inaccurate value of the total amount of Py chemisorbed on the zeolite disc. As mentioned previously, an unknown quantity of Py can be adsorbed on the walls of the IR cell leading to the erroneous determination of the amount of the probe molecule interacting with each type of acid sites, which would strongly affect the calculations [40,47]. (It should be noted that the application of AGIR methodology in this work virtually eliminates this problem.) Thirdly, the principal assumption of this model is that only one type of BAS and one type of LAS are present within the zeolite structures. However, in practice, this is not true in most cases. For instance, a significant number of defect sites are present in zeolite BEA, such as Si-OH and Al-OH groups with weak or moderately strong Brønsted acidity, while the nature of Lewis acidity is still under discussion. Hence, the molar absorption coefficient values presented in Table S5 show particularly poor statistics for zeolite BEA, even though the first two limitations of this model have been minimised in this work. For all these reasons, the quantitative evaluation of acidity in solid catalysts containing a range of both BAS and LAS may be associated with significant errors and should be carried out with a great deal of care.

Practical recommendations.

The following suggestions, aiming to enhance the quality of FTIR characterisation of acid sites in zeolites and to ensure its quantitative nature, can be made.

For the preparation of the self-supported disks, the amount of the sample should be kept between 5 and 15 mg per cm² and preferably no higher than 10 mg per cm², to ensure both good signal to noise ratio and linearity between absorbance and surface concentration.

The load applied when pressing the samples should not exceed 0.5 tonne per cm² in order to avoid possible incomplete activation and structural degradation of the zeolite. The design of the IR cell for kinetic type measurements and other experimental parameters, e.g. the activation temperature and the number of repeat samples, should be carefully considered and tested.

Physisorbed Py should be removed, its evacuation should be conducted preferably at 200°C and should be monitored spectroscopically. The desired spectral resolution should be chosen with care (the commonly used resolution of 4 cm⁻¹ is recommended), and the intensity of infrared bands of Py-L and Py-B complexes should be measured as peak area, rather than peak height.

The effects of the sample temperature on the measurements of the position and intensity of infrared bands ($\sim 10\%$ decrease per 100°C difference) should be taken into account to enable a quantitative comparison with the literature data. As the values of (Py-B) are affected by the zeolite structure and composition, additional calibration and cross-correlation with other analytical techniques may be required, especially for solids containing both BAS and LAS. In general, such calibrations should be performed separately for different types of zeolites.

Finally, we suggest that a systematic indication of the following elements in experimental reports would be a good practice: (i) amount of zeolite per unit disc area (e.g. 10 mg cm^{-2}), (ii) pressure applied for the preparation of the disc (e.g. 0.5 tonne cm^{-2}), (iii) conditions of activation of the sample prior adsorption (e.g. under vacuum at 450°C for 5 hours), (iv) conditions of pyridine adsorption (e.g. 150°C , 0.5 mbar equilibrium pressure), (v) precautions taken to remove physisorbed species (e.g. evacuation at 200°C), (vi) spectral resolution (e.g. 4 cm^{-1}), (vii) sample temperature during the acquisition of spectra (e.g. 30°C).

5. Conclusions

This study presents a detailed methodology for accurate calculation of the integrated molar absorption coefficients of Py complexes, (Py-B) and (Py-L) , which are essential for quantitative characterisation of the acidic properties of zeolites. This work demonstrates that the Beer-Lambert-Bouguer law is valid for IR characterisation of zeolites and makes it evident that careful design of the experimental procedures is essential for quantitative FTIR measurements. The obtained values of the molar absorption coefficients presented here can be used directly to determine the number of acid sites in different zeolites if the experimental conditions match those utilised in our work. If the conditions are different, then the correlations and detailed quantitative data provided in this paper and in Supporting Information should be sufficient to make the necessary adjustments.

The direct quantitative measurements of the molar absorption coefficients using AGIR experiments demonstrate that the values of (Py-B) depend on the zeolite structure, increasing in the order $\text{ZSM-5} \approx \text{BEA} < \text{MOR} < \text{FAU}$, which could be linked to the changes in Si/Al ratio, the acid site strength and confinement effects, all of which can alter the localised electrostatic field around adsorbed Py species, thus affecting the magnitude of the transient dipole moment of protonated Py that governs the value of (Py-B) . In contrast, the transient dipole moment of Py molecules coordinated to LAS (rather than protonated) appears to be influenced significantly less. Indeed, the (Py-L) values are almost the same, within the error of the measurements, for different zeolite structures and even for Py interacting with Na^+ and Ca^{2+} cations. Additionally, a clear correlation is established between the temperature of the infrared measurements and the magnitude of the molar absorption coefficients, which decrease by $\sim 10\%$ as the temperature increases by 100°C , and a similar effect is observed for other vibrating species. The unusual attenuation of the intensity of Py-

B peak by physisorbed Py, which apparently reduces the value of (Py-B), has been clearly identified. Likewise, the effects of the experimental methodology, e.g. the spectral resolution, have been evaluated and quantified.

Although quantum chemical calculations have not been planned as part of this research, it is clear that with the achieved quality of the experimental data there is a scope for computational modelling of the effects of the Si/Al ratio, confinement in micropores, the nature of acid sites, adsorption temperatures and physisorbed species on the magnitude of the transient dipole moment of various species present in zeolites. The experimental work can be also extended to the evaluation of other solid acids and catalytic materials containing different types of BAS and LAS as well as to the investigation of the effects of acid site strength and of the zeolite structure on the values of . The experimental (Py-B) and (Py-L) values obtained should significantly improve the accuracy of the quantitative analysis of acidic properties of zeolite-based catalysts using IR spectroscopy.

Acknowledgments

The authors thank ENSICAEN for the overall support for this research programme. We gratefully acknowledge Johnson Matthey PLC and Keele University (ACORN-2015 grant) for their support and funding provided for this work as the PhD studentship for C.F. M.J. thanks Keele University (ACORN-2018 grant), the Royal Society (International Exchanges grant IE160562) and the Newton Fund (Institutional Links grant 261867079) for supporting his PhD project. The authors thank Dr. D. Broom for providing a sample of NIST reference material RM8852, Prof. A.Y. Khodakov for providing a sample of alumina and Dr. A. Vicente for assistance with the MAS NMR measurements.

Supplementary Information

Supplementary data for this article can be found on-line at:

Conflict of interest.

The authors declare no competing financial interest.

References

- [1] K. Hadjiivanov. *Identification and characterization of surface hydroxyl groups by infrared spectroscopy*. Adv. Catal., 2014, 57, 99-318.
- [2] C. Morterra, G. Magnacca, V. Bolis. *On the critical use of molar absorption coefficients for adsorbed species: the methanol/silica system*. Catal. Today, 2001, 70, 43658

- [3] N.S. Nesterenko, F. Thibault-Starzyk, V. Montouillout, V. V. Yushchenko, C. Fernandez, J.P. Gilson, F. Fajula, I.I. Ivanova. *The use of the consecutive adsorption of pyridine bases and carbon monoxide in the IR spectroscopic study of the accessibility of acid sites in microporous/mesoporous materials*. Kinet. Katal., 2006, 47 (1), 40-48.
- [4] K. Góra-Marek, K. Tarach, M. Choi. *2,6-di-tert-butylpyridine sorption approach to quantify the external acidity in hierarchical zeolites*. J. Phys. Chem. C, 2014, 118, (23), 12266-12274.
- [5] T. Onfroy, G. Clet, M. Houalla. *Quantitative IR characterization of the acidity of various oxide catalysts*. Micro. Meso. Mater., 2005, 82, (162), 99-104.
- [6] B. Wichterlová, Z. Tvarukzová, Z. Sobalík, P. Sarv. *Determination and properties of acid sites in H-ferrierite. A comparison of ferrierite and MFI structures*. Micro. Meso. Mater., 1998, 24, 223-233.
- [7] P. Bazin, A. Alenda, F. Thibault-Starzyk. *Interaction of water and ammonium in NaHY zeolite as detected by combined IR and gravimetric analysis (AGIR)*. Dalton Trans., 2010, 39 (36), 8432-8436.
- [8] A.A. Gabrienko, I.G. Danilova, S.S. Arzumanov, L.V. Pirutko, D. Freude, A.G. Stepanov. *Direct Measurement of Zeolite Brønsted Acidity by FTIR Spectroscopy: Solid-State ¹H MAS NMR Approach for Reliable Determination of the Integrated Molar Absorption Coefficients*. Phys. Chem. C, 2018, 122, 25386-25395.
- [9] M. R. Basila, T. R. Kantner, K. H. Rhee. *The nature of the acidic sites on a silica-alumina. Characterization by infrared spectroscopic studies of trimethylamine and pyridine chemisorption*. J. Phys. Chem, 1964, 68 (11), 3197-3207.
- [10] M. R. Basila, T. R. Kantner. *The nature of the acidic sites on silica-alumina. A revaluation of the relative absorption coefficients of chemisorbed pyridine*. J. Phys. Chem., 1966, 70 (6) 1681-1682.
- [11] T. R. Hughes, H. M. White. *Study of the surface structure of decationized Y zeolite by quantitative infrared spectroscopy*. J. Phys. Chem., 1967, 71 (7), 2192-2201.
- [12] F. R. Cannings. *Acidic sites on mordenite. An infrared study of adsorbed pyridine*. J. Phys. Chem., 1968, 72 (13) 4691-4693.
- [13] M. Lefrancois, G. Malbois. *The nature of the acidic sites on mordenite. Characterization of adsorbed pyridine and water by infrared study*. J. Catal., 1971, 20, 350-358.
- [14] J. Datka. *Transformations of but-1-ene molecules adsorbed in NaHY zeolites studied by infrared spectroscopy*. J.C.S Faraday I., 1980, 76, 2437-2447.
- [15] J. Datka. *Dehydroxylation of NaHY zeolites studied by infrared spectroscopy*. J. Chem. Soc., Faraday Trans., 1, 1981, 77, 2877-2881.
- [16] J. Take, T. Yamaguchi, K. Miyamoto, H. Ohyama, M. Misono, *Brønsted site population on external and on internal surface of shape-selective catalysts*. Stud. Surf. Sci. Catal., 1986, 28, 495-502.
- [17] J. Datka, A. M. Turek, J.M. Jehng, I. E. Wachs. *Acidic properties of supported niobium oxide catalysts: An infrared spectroscopy investigation*. J. Catal., 1992, 135 (1), 186-199.

- [18] C. A. Emeis. *Determination of integrated molar extinction coefficients for infrared absorption bands of pyridine adsorbed on solid acid catalysts*. J. Catal., 1993, 141 (2), 347-354.
- [19] I. Kiricsi, C. Flego, G. Pazzuconi, W. O. Parker, Jr., R. Millini, C. Perego, G. Bellussi. *Progress toward understanding zeolite β acidity: An IR and ^{27}Al NMR spectroscopic study*. J. Phys. Chem., 1994, 98, 4627-463.
- [20] S. Khabtou, T. Chevreau, J. C. Lavalley. *Quantitative infrared study of the distinct acidic hydroxyl groups contained in modified Y zeolites*. Microporous Mater., 1994, 3, 133-148.
- [21] M. A. Makarova, K. Karim, J. Dwyer. *Limitation in the application of pyridine for quantitative studies of Brønsted acidity in relatively aluminous zeolites*. Microporous Mater., 1995, 4, 243-246.
- [22] M. Maache, A. Janin, J.C. Lavalley, E. Benazzi. *FT infrared study of Brønsted acidity of H-mordenites: heterogeneity and effect of dealumination*. Zeolites., 1995, 15, 507-516.
- [23] J. Datka, B. Gil, A. Kubacka. *Heterogeneity of OH groups in H-mordenites: Effect of dehydroxylation*. Zeolites., 1996, 17, 428-433.
- [24] M. Guisnet, P. Ayrault, C. Coutanceau, M. F. Alvarez, J. Datka. *Acid properties of dealuminated beta zeolites studied by IR spectroscopy*. J. Chem. Soc., Faraday Tran., 1997, 93 (8), 1661-1665.
- [25] B. Sulikowski, J. Datka, B. Gil, J. Ptaszynski, J. Klinowski. *Acidity and catalytic properties of realuminated zeolite Y*. J. Phys. Chem. B, 1997, 101, 6929-6932.
- [26] M. Guiset, P. Ayrault, J. Datka, *Acid properties of mazzite zeolites studied by IR spectroscopy*. Micro. Meso. Mater., 1998, 20, 283-291.
- [27] A. Taouli, A. Klemm, M. Breede, W. Reschtilowski. *Acidity investigations and determination of integrated molar extinction coefficients for infrared adsorption bands of ammonia adsorbed on acidic sites of MCM-41*. Stud. Surf. Sci. Catal., 1999, 125, 307-314.
- [28] E. Selli, L. Forni. *Comparison between the surface acidity of solid catalysts determined by TPD and FTIR analysis of pre-adsorbed pyridine*. Micro. Meso. Mater., 1999, 31, 129-140.
- [29] F. Thibault-Starzyk, B. Gil, S. Aiello, T. Chevreau, J. P Gilson. *In situ thermogravimetry in an infrared spectrometer: an answer to quantitative spectroscopy of adsorbed species on heterogeneous catalysts*. Micro. Meso. Mater., 2004, 67, 107-112.
- [30] K. Góra-Marek, M. Derewinski, P. Sarv, J. Datka. *IR and NMR studies of mesoporous alumina and related aluminosilicates*. Catal. Today, 2005, 101, 131-138.
- [31] K. Góra-Marek, J. Datka, S. Dzwigaj, M. Che. *Influence of V content on the nature and strength of acidic sites in VSi β zeolite evidenced by IR spectroscopy*. J. Phys. Chem. B., 2006, 110, 6763-6767.
- [32] B. Gil, G. Kosová, J. Cejka, *Acidity of MCM-58 and MCM-68 zeolites in comparison with some other 12-ring zeolites*. Micro. Meso. Mater., 2010, 129, 256-266.
- [33] I. S. Pieta, M. Ishaq, R. P. K. Wells, J. A. Anderson. *Quantitative determination of acid sites on silica-alumina*. Appl. Catal. A., 390 (2010) 127-134.
- [34] J. M. R. Gallo, C. Bisio, G. Gatti, L. Marchese, H. O. Pastore. *Physicochemical characterization and surface acid properties of mesoporous [Al]-SBA-15 obtained by direct synthesis*. Langmuir., 2010, 26 (8), 5791-5800.

- [35] E. J. M Hensen, D. G. Poduval, V. Degirmenci, D. A. J. M, Ligthart, W. Chen, F. Maugé, M. S. Rigutto, J. A Rob van Veen. *Acidity characterization of amorphous silica–alumina*. J. Phys. Chem. C., 2012, 116, 21416-21429.
- [36] J. W. Harris, M. J. Cordon, J. R. Di Iorio, J. C. Vega-Vila, F. H. Ribeiro, R. Gounder. *Titration and quantification of open and closed Lewis acid sites in Sn-Beta zeolites that catalyze glucose isomerization*. J. Catal., 2016, 335, 141-154.
- [37] I. Miletto, G. Paul, S. Chapman, G. Gatti, L. Marchese, R. Raja, E. Gianotti, *Chem. Eur. J.*, 2017, 23, 9952-9961.
- [38] K. A. Tarach, K. Góra-Marek, J. Martinez-Triguero, I. Melián-Cabrera, *Acidity and accessibility studies of desilicated ZSM-5 zeolites in terms of their effectiveness as catalysts in acid-catalyzed cracking processes*. Catal. Sci. Technol., 2017, 7, 858-873.
- [39] N. S. Gould, B. Xu. *Quantification of acid site densities on zeolites in the presence of solvents via determination of extinction coefficients of adsorbed pyridine*. J. Catal., 2018, 358, 80-88.
- [40] S. Bordiga, C. Lamberti, F. Bonino, A. Travert, F. Thibault-Starzyk. *Probing zeolites by vibrational spectroscopies*. Chem. Soc. Rev., 2015. 44 (20): 7262-7341.
- [41] P. Stelmachowski, S. Sirotin, P. Bazin, F. Maugé, A. Travert, *Speciation of adsorbed CO₂ on metal oxides by a new 2-dimensional approach: 2D infrared inversion spectroscopy (2D IRIS)*. Phys. Chem. Chem. Phys. 2013, 15, 9335-9342.
- [42] B. Moulin, L. Oliviero, P. Bazin, M. Daturi, G. Costentin, F. Maugé, *How to determine IR molar absorption coefficients of co-adsorbed species? Application to methanol adsorption for quantification of MgO basic sites*. Phys. Chem. Chem. Phys. 2011, 13, 10797-10807.
- [43] F. Vilmin, P. Bazin, F. Thibault-Starzyk, A. Travert, *Speciation of adsorbates on surface of solids by infrared spectroscopy and chemometrics* *Analytica Chimica Acta*. 2015, 891, 79-89.
- [44] S. Turner, J.R. Sieber, T.W. Vetter, R. Zeisler, A.F. Marlow, M.G. Moreno-Ramirez, M.E. Davis, G.J. Kennedy, W.G. Borghard, S. Yang, A. Navrotsky, B.H. Toby, J.F. Kelly, R.A. Fletcher, E.S. Windsor, J.R. Verkouteren, S.D. Leigh, *Characterization of chemical properties, unit cell parameters and particle size distribution of three zeolite reference materials: RM 8850 - zeolite Y, RM 8851 - zeolite A and RM 8852 - ammonium ZSM-5 zeolite*, Micro. Meso. Mater., 2008, 107, 252-267.
- [45] L. M. Parker, D. M. Bibby, G. R. Burns. *Fourier-transform infrared study of pyridine sorbed on zeolite HY*. J. Chem. Soc. Faraday Trans., 1991, 87 (19), 3319-3323.
- [46] A. Zecchina, L. Marchese, S. Bordiga, C. Paze, E. Gianotti. *Vibrational spectroscopy of NH₄⁺ ions in zeolitic materials: an IR study*. J. Phys. Chem. B, 1997, 101, 6929-6932.

[47] A. Popov, E. Kondratieva, J. M. Goupil, L. Mariey, P. Bazin J.-P. Gilson, A. Traver, F. Maugé. *Bio-oils hydrodeoxygenation: Adsorption of phenolic molecules on oxidic catalyst supports*. J. Phys. Chem. C., 2010, 114, 15661- 15670.